

Alfvén Wing-Like Structures in Titan's Magnetotail During T122-T126 Flybys

 Konstantin Kim^{1,2} , Niklas J. T. Edberg¹ , Jan-Erik Wahlund¹ , and Erik Vigren¹ 
¹Swedish Institute of Space Physics, Uppsala, Sweden, ²Department of Physics and Astronomy, Uppsala University, Uppsala, Sweden

Key Points:

- During the T123 and T124 Titan flybys an Alfvén wing-like structure was detected
- An analysis of all tailside flybys reveals a clear bipolar draping of the magnetic field around Titan
- Magnetic field and plasma density are analyzed during T122-T126 to estimate the escape rate in an magnetohydrodynamics regime

Supporting Information:

Supporting Information may be found in the online version of this article.

Correspondence to:

K. Kim,
konstantin.kim@irfu.se

Citation:

Kim, K., Edberg, N. J. T., Wahlund, J.-E., & Vigren, E. (2024). Alfvén wing-like structures in Titan's magnetotail during T122-T126 flybys. *Journal of Geophysical Research: Space Physics*, 129, e2023JA032265. <https://doi.org/10.1029/2023JA032265>

Received 10 NOV 2023

Accepted 3 JUN 2024

Author Contributions:

Conceptualization: Konstantin Kim, Niklas J. T. Edberg

Formal analysis: Jan-Erik Wahlund, Erik Vigren

Investigation: Konstantin Kim, Niklas J. T. Edberg, Jan-Erik Wahlund

Methodology: Niklas J. T. Edberg, Jan-Erik Wahlund

Software: Konstantin Kim

Supervision: Niklas J. T. Edberg, Jan-Erik Wahlund, Erik Vigren

Validation: Erik Vigren

Visualization: Konstantin Kim

Writing – original draft:

Konstantin Kim, Niklas J. T. Edberg

Writing – review & editing:

Konstantin Kim, Niklas J. T. Edberg, Jan-Erik Wahlund, Erik Vigren

©2024. The Author(s).

This is an open access article under the terms of the [Creative Commons Attribution License](https://creativecommons.org/licenses/by/4.0/), which permits use, distribution and reproduction in any medium, provided the original work is properly cited.

Abstract In this paper, we study Titan's magnetotail using Cassini data from the T122-T126 flybys. These consecutive flybys had a similar flyby geometry and occurred at similar Saturn magnetospheric conditions, enabling an analysis of the magnetotail's structure. Using measurements from Cassini's magnetometer (MAG) and Radio and Plasma Wave System/Langmuir probe (RPWS/LP) we identify several features consistent with reported findings from earlier flybys, for example, T9, T63 and T75. We find that the so-called 'split' signature of the magnetotail becomes more prominent at distances of at least 3,260 km ($1.3 R_T$) downstream of Titan. We also identify a specific signature of the sub-alfvenic interaction of Titan with Saturn, the Alfvén wings, which are observed during the T123 and T124 flyby. A coordinate transformation is applied to mitigate variations in the upstream magnetic field, and all the flybys are projected into a new reference frame—aligned to the background magnetic field reference frame (BFA). We show that Titan's magnetotail is confined to a narrow region of around $\sim 4 R_T Y_{BFA}$. Finally, we analyze the general draping pattern in Titan's magnetotail throughout the TA to T126 flybys.

1. Introduction

Saturn's magnetosphere in the vicinity of Titan's orbit exhibits a complex structure and is a major source of the variability seen at Titan, that is, induced magnetosphere, ionosphere, and magnetotail (e.g., Galand et al., 2014; Wahlund et al., 2014). The magnetic field lines are stretched out radially outwards from Saturn at Titan's orbit of about $20 R_S$ ($1 R_S \approx 60,268$ km, $1 R_T = 2,574.7$ km), forming a magnetodisk region filled with ions from both Saturn and its moon Enceladus. As a result of the solar wind interaction with Saturn's magnetosphere, the magnetodisk is bent, most notably on Saturn's dayside (e.g., Arridge et al., 2008). Due to the rotation axis of Saturn being tilted and the magnetosphere rotating at a speed faster than Titan's orbital motion, Titan is periodically exposed to the low- β plasma of magnetospheric lobes and high- β plasma in the magnetodisk. Altering the configuration and composition of the upstream magnetic field and corotating plasma eventually leads to the variable plasma environment of Titan. Several classifications of Titan's plasma environment have been performed, which take into account Saturn's magnetodisk modulation and are based on measurements of the ion and electron plasma, energetic particles, and magnetic field properties (e.g., Garnier et al., 2010; Kabanovic et al., 2017; Morooka et al., 2009; Németh et al., 2011; Regoli et al., 2018; Rymer et al., 2009; Simon et al., 2010b; Smith & Rymer, 2014).

Most of the time Titan is well embedded into Saturn's magnetosphere, but it can be exposed to the magnetosheath and in extreme cases even to the solar wind, when the magnetosphere of Saturn experiences enhanced solar wind pressure and/or is subjected to coronal mass ejection impacts (e.g., Bertucci et al., 2008; Bertucci et al., 2015; Burne et al., 2023; Edberg et al., 2013; Feyerabend et al., 2016; Wei et al., 2011). The presence of Titan in the magnetosheath deforms Saturn's bowshock and leads to a sophisticated structure of a foreshock region, for example, Omidi et al. (2017) and Burne et al. (2023). The exposure of Titan to the supermagnetosonic solar wind flow is the only way for Titan to create a bowshock, similar to Mars and Venus. The interaction of Titan's ionosphere, created mainly by extreme ultraviolet radiation on the atmosphere, with the incoming flow is modulated by the solar direction relative to the local normal and magnetospheric conditions (e.g., Ågren et al., 2009). The incoming corotating plasma is deflected around Titan and is convected tailward. On the ramside, the magnetic field is piled up creating an induced magnetosphere together with ionospheric currents (Ågren et al., 2011), and the magnetic field lines are draped around Titan toward the wakeside. For an unmagnetized body, like Titan, in a sub-magnetosonic flow, an Alfvén wing-type structure is expected to appear, coupling the magnetosphere of Saturn with Titan's ionosphere via a system of field-aligned currents. This coupling is

theoretically described in the case of Galilean moons by Neubauer (1998). An extended region of stretched-out magnetic field lines with ionospheric material from Titan, known as a magnetotail is formed. A similar coupling between Saturn's moons and Saturn's magnetosphere has been observed during close Cassini flybys of Enceladus (e.g., Gurnett et al. (2011); Engelhardt et al. (2015)).

As Titan is embedded into the sub-magnetosonic flow of Saturn's magnetospheric plasma and given Titan's dense atmosphere, the Alfvén wing interaction feature is expected to be reminiscent of interactions at the Jovian moons Io and Ganymede. The straightforward derivation from the magnetohydrodynamics (MHD) equation by Neubauer (1980) shed light on how Io interacts with the Jovian magnetosphere. In this model, Jovian magnetic field perturbations during the interaction with Io's plasma environment create Alfvén waves, propagating from Io along the magnetic field lines to Jupiter's auroral ionosphere. If the same framework is applied to Titan, the model suggests the bending of Saturn's magnetic field around Titan and further convection down the wake, and generating Alfvén wings. In the case of strong interaction, Saturn's magnetosphere and Titan's plasma environment are coupled via field-aligned currents in Saturn's magnetosphere, which is then closed in Titan's ionosphere by Hall and Pedersen currents. The cone angle of the Alfvén wing can be estimated as $\tan \theta = V/V_A$, where V_A is the Alfvén velocity, and V is the bulk velocity of plasma.

Cassini made a total of 126 close flybys, exploring Titan's plasma environment. However, most of the flybys occurred outside of the wake or magnetotail. The first Cassini observations of Titan's magnetotail revealed an expected draped magnetic field structure, confirming Voyager one observations and simulations (Backes et al., 2005). It was also noticed that Titan lacked an intrinsic magnetic field. The following flybys TB and T3 were also suitable for analyzing the magnetotail (Neubauer et al., 2006). Among one of the most extensively studied flybys, T9, plasma and magnetic field parameters were analyzed in a number of papers (e.g., Bertucci et al., 2007, and references therein). In Bertucci et al. (2007) the magnetic field structure was analyzed. It was found that at a distance of $\sim 5 R_T$ a well-developed bipolar structure associated with the magnetotail lobes was separated by a neutral current sheet. The analysis of cold plasma in the same region by Wei et al. (2007) revealed two spatially separated outflow regions or a so-called "split" tail signature. The analysis of ion measurements by Szego et al. (2007) explained an observed "split" signature as the crossing of the escaping ions along the magnetic field lines in the distant tail region of Titan. Multi-species hybrid simulation by Modolo et al. (2007) explained the observed asymmetry in electron densities by the dayside/nightside asymmetry in the electron production rate of Titan. This suggests that during the first crossing of a split tail structure, the plasma density was higher due to its connectivity to the dayside Titan's ionosphere. The hybrid simulation of Kallio et al. (2007) suggests that sub-corotating flow was most likely dominated by heavy ions being magnetically connected to the sunlit ionosphere during the T9 flyby. This is consistent with Modolo et al. (2007). A follow-up paper by Coates et al. (2012) focuses on the distant tail flybys T9, T63, and T75 from the point of view of plasma measurements. It was found that heavy ions ($m/q \sim 16$ and 28 amu) and light ions ($m/q \sim 1-2$ amu) were streaming down the tail through filaments at an established variable mass loss rate of ~ 9 , ~ 4 and $\sim 1.6 \times 10^{25}$ amu s^{-1} for T9, T63 and T75, respectively. A study of the same flybys by Feyerabend et al. (2015) using the hybrid simulation focused on the kinetic features of the ion tail. The observed split signature of the ion tail was explained as a result of the ion escape pattern. The pressure gradients increased the effective size of an obstacle, allowing escaping ions to shape a cone structure. The escaping ions form filaments, the density and location of which depend on the upstream flow parameters. In Edberg et al. (2011) the T55-T59 Titan's tail/nightside were analyzed and a plume of escaping ionospheric plasma was observed. It was proposed that the observed structured atmospheric escape can be a result of ambipolar diffusion, magnetic pumping moment, or dispersive Alfvén waves. Simon et al. (2014) summarized all Titan's mid-range tail flybys from TA to T82, combining magnetic field measurements in this region into one coherent picture, finding, for example, that the magnetotail is confined to a region within $\pm 3 R_T$ from the $Y = 0$ plane in the draping frame (see Section 2). The transition from the northern to southern magnetotail lobes typically is observed at a distance of $\leq 2.5 R_T$.

This paper focuses on the last five Titan flybys, T122-T126, analyzing magnetotail geometry and properties of that plasma region. These flybys are of particular interest because the flyby trajectories cover similar regions in Titan's magnetotail in a similar ambient plasma environment. We seek also, by combining our findings with results from studies of other Titan flybys, to determine common patterns in the draping of Titan's magnetotail. The paper is structured as follows: in Section 2 we introduce reference frames used in this paper. Then we proceed with the description of the flyby trajectories in Titan's wake during T122-T126 in Section 3.1. In Section 3.2 we provide examples of the observed magnetic field structures, associated with the Alfvén wings and elaborate on its

evolution in Section 3.3. In Section 3.4 we use all available flybys to infer the general draping pattern from TA to T126. Finally, in Section 4 we conclude with the discussion.

2. Methods and Coordinate Frames

The Cassini spacecraft had a rather comprehensive instrument payload to measure magnetic fields (Dougherty et al., 2004), cold plasma characteristics using the Langmuir probe (LP) (Gurnett et al., 2004) and the more energetic plasma populations using the Cassini Plasma Spectrometer (CAPS) instrument (Young et al., 2004). The measurements of cold ionospheric plasma density and temperature are estimated by LP bias potential sweep (later in the text mentioned as the LP mode). By sweeping the bias potential from negative to positive voltages (± 32 V in the magnetosphere, ± 4 V in the ionosphere), the LP either attracts or repels charged particles. The resulting current is then fitted to retrieve plasma density and temperature (e.g., Chatain et al., 2021; Gustafsson & Wahlund, 2010; Morooka et al., 2011; Shebanits et al., 2016). In addition, “20 Hz” fixed voltage-bias mode (when the bias voltage is fixed and the current is sampled at 20 Hz) and upper-hybrid resonance (from the electric field fluctuations spectrum) frequency f_{UH} are used to determine local electron density. Unfortunately, in 2012 the CAPS plasma measurements of electrons and ions ended, following a power anomaly. It is thus not possible for us to make a “complete comparison” of the plasma environments encountered during the last five flybys with those encountered during, for example, T9, T63, and T75 as reported by Coates et al. (2012).

To account for the upstream variations of the magnetic field, the measured by magnetometer (MAG) magnetic field data in a corotating frame is transformed into the aligned to the background magnetic field (BFA) reference frame. In the corotating frame (TIIS) X_{TIIS} is along the ideal corotation direction, Y_{TIIS} toward Saturn and Z_{TIIS} completes the right-handed system. To define the field-aligned direction, the inbound and outbound magnetic fields are averaged around ± 1 hr before and after the closest approach. Fortunately for all the T122-T126 flybys Titan's plasma environment remains in the northern lobe steady with minor perturbations from the plasma sheet based on the classification of Kabanovic et al. (2017). Given that, we can construct a steady field-aligned coordinate system (BFA) orienting Z_{BFA} parallel to the averaged upstream magnetic field direction, X_{TIIS} is parallel to the ideal flow direction, and $Y_{BFA} = -X_{TIIS} \times Z_{BFA}$. However, this system is not orthogonal, thus X_{BFA} is redefined as $X_{BFA} = Y_{BFA} \times Z_{BFA}$, and each basis vector is a column vector. The transform matrix from the local Titan's interaction frame (TIIS) to a draping frame $T_{TIIS \rightarrow BFA} = [X_{BFA} \ Y_{BFA} \ Z_{BFA}]^T$. After the transformation, deviations from the background magnetic field direction in Titan's wake are associated either with the magnetotail or local disturbances of Saturn's magnetosphere.

Instead of a BFA reference frame, the so-called draping reference frame was used in the previous studies (e.g., Bertucci et al., 2007; Neubauer et al., 2006). The only difference between these two reference frames is the Z-axis, which in the case of the draping reference frame is anti-parallel to the magnetic field. In this paper, we use the background magnetic field direction as a natural reference direction when analyzing Titan's magnetotail and the coupling of Titan's plasma environment with Saturn's magnetosphere. The same transformation was applied on all the flybys to infer the draping pattern of the magnetic field. In this case, an additional criterion must be introduced constraining the maximum angle α between the inbound and outbound magnetic field. If the angle $\alpha \leq 20^\circ$, then this flyby cannot be transformed into a steady reference frame, since the deviations might originate from a different source, for example, a transition from the northern lobe to the plasma sheet. The 20° threshold is simply chosen as an arbitrary, but rather conservative, upper limit. The result of the verification is shown in Section 3.2.

3. Observations

3.1. Flyby Geometry and Upstream Conditions During T122-T126 Flybys

In Figure 1 the flyby geometry of Cassini during T122-T126 is shown in cylindrical projection ($X_{TIIS}, \rho_{TIIS} = \sqrt{X_{TIIS}^2 + Y_{TIIS}^2}$; $X_{ecl}, \rho_{ecl} = \sqrt{X_{ecl}^2 + Y_{ecl}^2}$). The series of consecutive flybys with similar flyby geometry occurred in slightly different SLT (see Table 1), approaching Titan from the wakeside to the ramside (see Figure 1d). The spacecraft moved from the dayside to the nightside (see Figure 1e). The first four flybys were progressively moving further away in the wakeside direction. Then in the last flyby, the geometry changes in the opposite direction, getting closer to Titan. The closest approach altitude ranged from 1,585 km ($0.615 R_T$) to 3,160 km ($1.23 R_T$), or in particular: T122—1,698 km ($0.66 R_T$), T123—1,773 km ($0.68 R_T$), T124—1,585 km

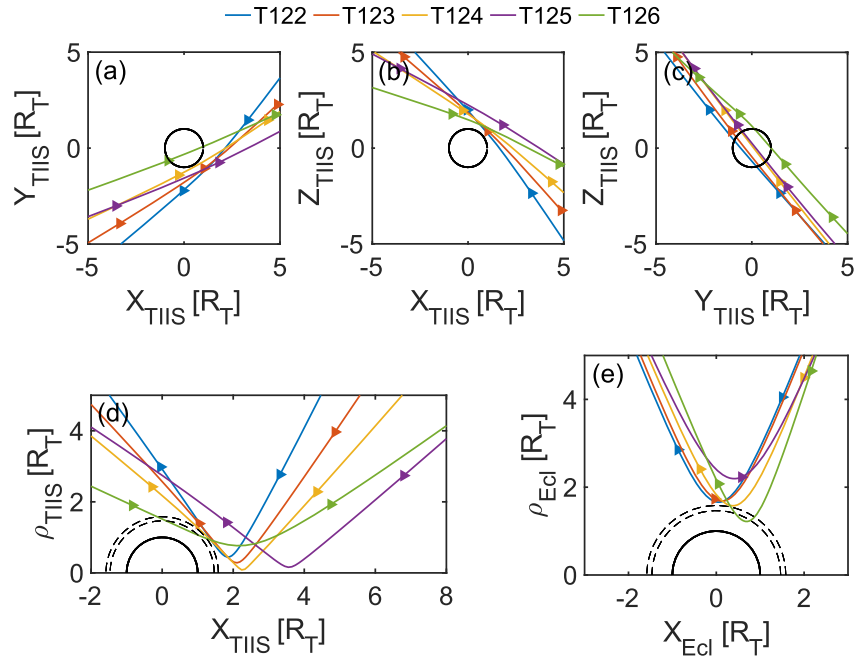


Figure 1. The Cassini's flyby trajectory during T122-T126: (a–c) the projections of the flyby trajectory in TIIS frame (X is along the ideal corotating direction), (d and e) are cylindrical projections of the flyby trajectory in TIIS and ecliptical frames (X is pointing to the Sun). The area between the dashed line around Titan indicates the collision-dominated part of the ionosphere at altitudes of 1,200–1,500 km (e.g., Ågren et al., 2009).

(0.62 R_T), T125—3,160 km (1.23 R_T), T126—980 km (0.38 R_T). The spacecraft velocity throughout the flybys remained the same: ~ 6 km/s.

To describe the magnetotail configuration, Titan's upstream conditions are first assessed during T122-T126. In Table 1 the magnetic field data is presented for the flybys T122-T126 together with the classification of upstream conditions according to Kabanovic et al. (2017) in the last column. The classification scheme follows the previously described scheme in Simon et al. (2010a) and is based on the calculation of the magnetic field direction. Depending on how stretched out the magnetic field lines are on average during ± 3 hr around the closest approach with Titan, several categories of the ambient plasma environment are categorized. These categories represent Saturn's magnetodisk current sheet (Sh) and magnetospheric lobes (L), the upper subscript denotes northern or southern magnetospheric lobes, and the lower subscript—the interference with another category. For example, L_{Sh}^S corresponds to the southern magnetospheric lobe of Saturn (as the averaged radial component B_ρ of the averaged magnetic field B is dominant, i.e., $|B_\rho|/|B| < 0.6$) with the interference of magnetodisk current sheet-type fields. The interference means in this case, that the averaged radial component B_ρ of the averaged magnetic field is strong, but possesses a high level of shorter-scale fluctuations δB_ρ , that is, $0.05 \leq |\delta B_\rho|/|B| < 0.2$.

Table 1
Cassini Tail Flybys Characteristics

Flyby number	Crossing time	$\langle \mathbf{B}_{inb} \mathbf{B}_{out} \rangle$ [deg]	$ \mathbf{B}_{inb} / \mathbf{B}_{out} $	SLT	SSL	Class. In-out
T122	2016/08/10 08:11–08:52	10.12	0.89	1.9	26.4	$L^N - L^N$
T123	2016/09/27 03:59–04:41	2.96	0.89	1.8	26.5	$L^N - L^N$
T124	2016/11/13 23:32–24:18	6.15	0.98	1.7	26.6	$L^N - L^N$
T125	2016/11/29 03:59–04:41	20.81	0.48	1.6	26.6	$L_{Sh}^N - L_{Sh}^N$
T126	Deep ionosphere	6.71	1.59	1.0	6.7	$L_{Sh}^N - Sh_{L^N}$

Note. The crossing time of the magnetotail-like magnetic field is in column 1. The angle between the inbound and outbound magnetic field $\langle \mathbf{B}_{inb} \mathbf{B}_{out} \rangle$ and $|\mathbf{B}_{inb}|/|\mathbf{B}_{out}|$ are in columns 2 and 3. The Saturn Local Time (SLT) and sub-solar longitude (SSL) are in columns 4 and 5. The classified background environment is in column 6.

The second column shows a crossing time of the region where the deviations from the background magnetic field direction are the most significant. The angle between the inbound and outbound magnetic field and the magnitude ratio is shown in columns 3 and 4, and indicate how much the magnetic field changes from inbound to outbound. The orbital phase of Titan with respect to Saturn and sub-solar longitude (SSL) are provided in columns 5 and 6. As can be seen, the magnetic field on both inbound and outbound legs in all flybys doesn't change its direction (minimum rotation angle is 2.9° , and maximum is 20.8°). At the same time, the magnitude of the magnetic field changes throughout the flybys. From T122 to T124 the inbound magnetic field is slightly smaller than the outbound magnetic field. During T125 the inbound magnetic field is only about half of the outbound magnetic field magnitude. Finally, T126 shows a stronger inbound magnetic field. Overall, the magnetic field environment corresponds to the northern lobe of Saturn's magnetosphere with increasing perturbations from the plasma sheet region during the final two flybys. Regarding the particle environment classification, Rymer et al. (2009) showed that when Titan is exposed to one of Saturn's magnetospheric lobes, the electron's energy peaks from 150 to 820 eV. The classification of ion distribution functions by Németh et al. (2011) usually corresponds well with Rymer et al. (2009), and thus when the environment is classified as Saturn's magnetospheric lobe, the ion distribution function has two peaks, the light (protons and alphas mostly) ion peak at around 400–600 eV, and highly suppressed heavy (water group) ions peak at around 4,400 eV. It is worth mentioning that the proposed classifications utilize different time scales (for in-detail comparison of aforementioned classification results, see Arridge et al. (2011)).

3.2. Examples: T122 and T124 Flybys

As described earlier in Section 2, to mitigate the possible influence of the upstream magnetic field variations, the magnetic field data was transformed into a BFA reference frame. As an example of such transformation, Figure 2 shows the magnetic field and electron density during the T122 flyby. The spacecraft altitude is shown on top of the magnetic field data as a dot-dashed line in panel (a) and the dashed vertical line indicates the closest approach time (the closest approach distance is 1,697 km). The first panel (a) presents the initial magnetic field data in the TIIS reference frame. Inbound and outbound intervals are arbitrarily chosen well outside of the interaction region and averaged (highlighted blue-shaded area in panel (a)). The duration of these time intervals was selected so the magnetic field was stable and far from the closest approach, at approximately ± 1 hr. The averaged inbound and outbound magnetic fields were compared. If the angle between them had been large it would not have been possible to define a background magnetic field direction. Luckily in the considered flybys, this angle did not change much (less $\sim 10^\circ$), and so in all cases, a background magnetic field direction could be set and the field-aligned reference frame could be constructed following the procedure outlined in Section 2.

In Figure 2 panel (b) the result of that transformation is shown. As expected, the non-background magnetic field components of the magnetic field ($B_{x,BFA}$ and $B_{y,BFA}$) are negligible and oscillate around zero value outside of the interaction region. At approximately 08:10 UTC (stands for Universal Time Coordinated) the magnetic field direction starts to deviate from the background magnetic field direction. From 08:10 to 08:50 the non-background magnetic field component $B_{x,BFA}$ is the largest component as the spacecraft passes through bent-around Titan magnetic field lines, indicating a crossing of one of the magnetotail lobes. The bipolar structure of the magnetic field with the well-developed neutral current sheet in between magnetotail lobes is consistent with previously reported flybys, for example, T9 (e.g., Bertucci et al., 2007). The electron density is shown in panel (c) with three measurement modes: (red) LP sweeps, (green) upper-hybrid resonance frequency f_{UH} , and (blue) LP fixed voltage-bias 20 Hz mode (for details see Section 2). The electron density in the magnetotail lobes increases up to 100 cm^{-3} . An electron density spike is seen at the same time as a neutral current sheet is observed. The split signature which is discussed as a common feature of Titan's magnetotail is not observed during this flyby. However, this flyby is closer to Titan compared to other flybys in this study. The electron temperature ranges from 0.1 to 1 eV throughout the duration of the flyby. The spacecraft potential remains negative and follows an opposite trend to that of the electron temperature to the electron temperature.

In Figure 3, another example of a flyby, T124, through Titan's magnetotail region is shown. The upstream magnetic field does not show any significant variation between the inbound and outbound legs. Between 23:40–23:45 UTC and 23:55–00:00 UTC, bipolar signatures of the magnetotail lobes are observed. The magnetotail lobes are separated in time, which is different compared to T122 (see Figure 2), where the transition between magnetotail lobes was continuous. The electron density also shows two bi-lobe enhancements which correspond to the magnetotail lobe in the inbound leg around 23:41 and 23:46 UTC, and the topside ionosphere and

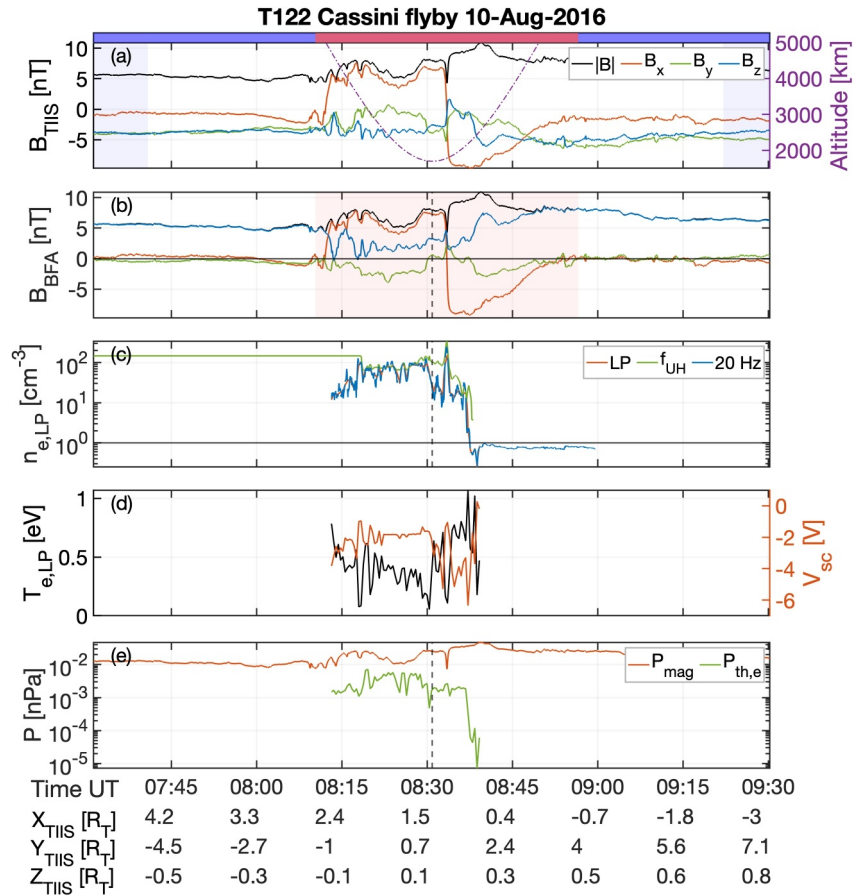


Figure 2. An example of the Cassini measurements during T122. From top to bottom: measured magnetic field \mathbf{B} in TIS coordinates (a) and transformed into BFA reference frame (b), electron density $n_{e,LP}$ (c), electron temperature $T_{e,LP}$ and spacecraft potential V_{sc} on the right axis (d), magnetic (red) and thermal (green) electron pressure P . The thermal pressure is estimated only using Langmuir probe electron density and temperature. The colorbar on top of the figure corresponds to Saturn's magnetosphere outside interaction region (blue) and Titan's magnetotail (red) regions. The vertical dashed lines in panels (a–c) indicate the closest approach time. In panel (a) the shaded red-colored regions are time intervals both inbound and outbound where the magnetic field is averaged and in addition, on the right axis the spacecraft altitude is superposed.

magnetotail in the outbound leg. Another difference is the presence of a current sheet in the inbound leg, observed at the boundary of the magnetotail lobe during T124. This could correspond to the field-aligned current or surface current, of one of the lobes (to be discussed in Section 4). The presence of cold ionospheric electrons is indicated both by drops of the electron temperature and jumps of the spacecraft potential (which is negative during the whole flyby) from ~ -5 V up to ~ -1 V.

The observed fluctuations of the magnetic field during this current sheet crossing are shown in Figure 4. In panel (a) the magnetic field in the BFA reference frame is shown (solid). To infer the fluctuating component of the magnetic field, the smoothed magnetic field components were individually subtracted from the measured magnetic field. The fluctuating component of the magnetic field δB is shown in panel (b). The peak fluctuations are observed at around 23:41:58 UT ($\delta B_x \approx -1.4$ nT, $\delta B_z \approx 0.6$ nT) and around 23:42:22 UT ($\delta B_x \approx 0.7$ nT, $\delta B_y \approx 0.9$ nT and $\delta B_z \approx -1.4$ nT) and are indicated by the vertical line. The angle β between the background and fluctuating magnetic field in panel (c) is invariant regardless of the reference frame and therefore the reference frame remains the BFA. The red-shaded area shows how β changes when the length of the smoothing time interval changes from 0.6 to 3.6 min. The values are chosen so we smooth out fluctuations on smaller scales. Around the peak magnetic field fluctuations, the fluctuations are nearly transverse to the background magnetic field.

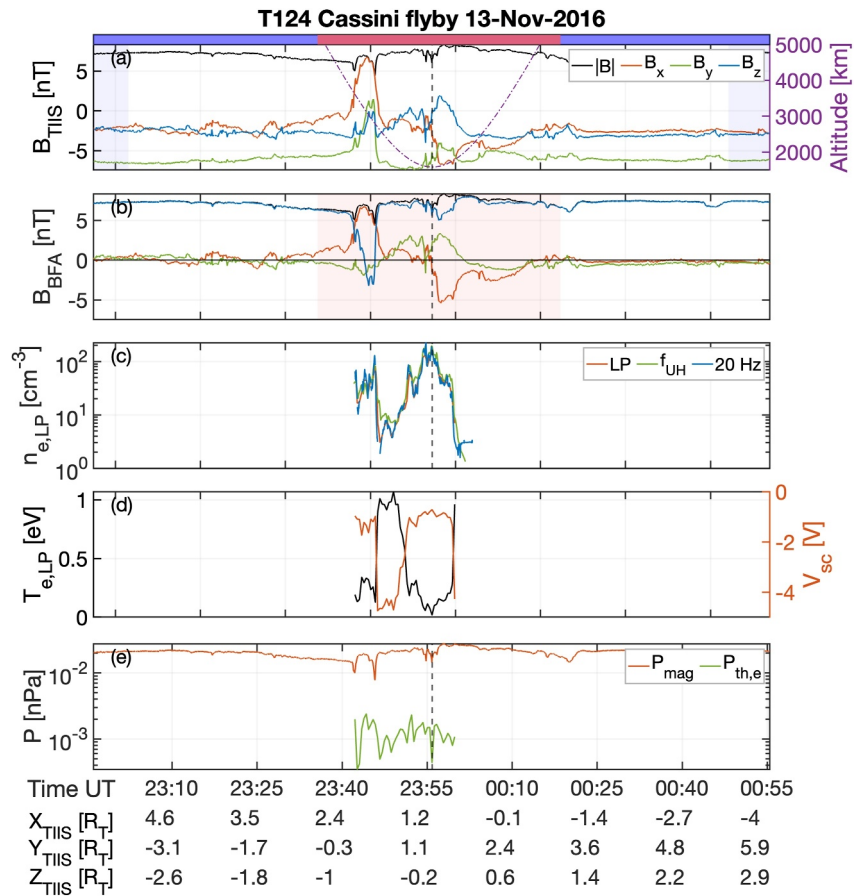


Figure 3. The same format as in Figure 2.

3.3. Evolution of the Non-Background Magnetic Field Component of the Magnetic Field

The geometry of the selected flybys T122-T125 allows Cassini to cover different regions of the magnetotail. All of those flybys were analyzed in the same way as described above for T122 and the results of the analysis are shown in Figure 5 (results from T126 are not displayed as T126 occurred in the deep ionosphere, where ionospheric currents are dominating). The X-axis shows the minutes before (<0) and after (>0) the closest approach. On the Y-axis the $B_{x,BFA}$ normalized to the magnitude of the magnetic field $|B|$ is shown for each of the flybys. The color represents the sign and the fraction of the total magnetic field associated with the $B_{x,BFA}$ or draping of the magnetic field. All the measurements are centered around the closest approach.

A few distinct regions are noticeable in Figure 5. The region with almost non-observable deviations in the $B_{x,BFA}$ component is referred to as Saturn's magnetosphere due to the observed nature of the magnetic field and observed beyond ± 20 (± 30 min for T125) from the closest approach. Then the region with the highest variation of the $B_{x,BFA}$ is referred to as Titan's magnetotail region. The bipolar magnetic field corresponds to the magnetotail lobes. The crossing of the magnetotail region is found in T122, T123, and T124 with a somewhat different pattern. The T122 flyby shows a confined magnetotail structure with a sharp transition of $\delta B_{x,BFA} \sim 16.3$ nT over $\Delta\tau \sim 2$ min interval between two magnetotail lobes, whereas T123 ($\delta B_{x,BFA} \sim 9.1$ nT over $\Delta\tau \sim 4$ min) and T124 ($\delta B_{x,BFA} \sim 11.7$ nT over $\Delta\tau \sim 13.5$ min) both display a split signature, that is, smooth and intermittent transitions between the magnetotail lobes. The T125 flyby possesses a split signature, but with a less pronounced bipolar magnetic field, which can be explained by partial crossing of one of the magnetotail lobes. The T126 flyby dives too low into the ionosphere, so the magnetic field does not reveal any lobe-like structures and is thus omitted. The magnitude of the magnetic field enhancement is found at ~ 7 – 10 nT at the closest approach and ~ 5 nT further away.

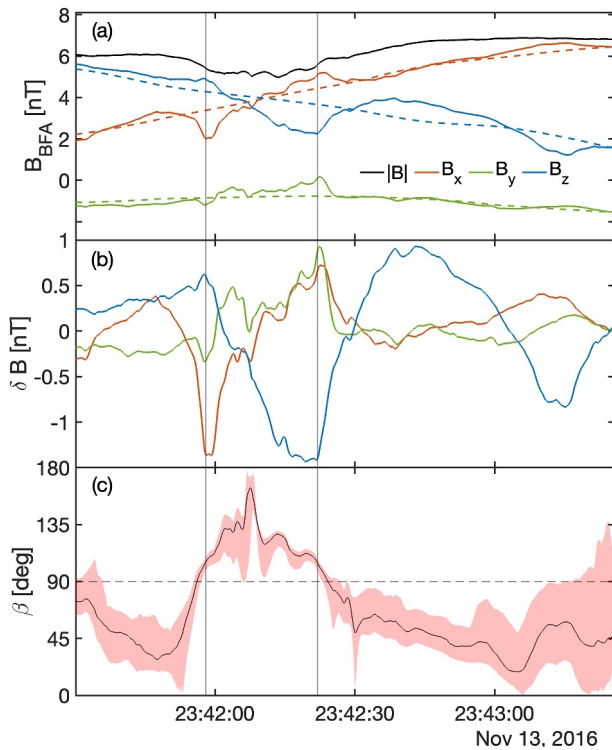


Figure 4. The fluctuations of the magnetic field \mathbf{B} during the current sheet crossing seen in T124 flyby: (a) the three components of the magnetic field (solid lines) and smoothed background (dashed lines) in the BFA reference frame, (b) the fluctuations of the magnetic field derived as a difference between the measured and smoothed magnetic field, (c) the angle β between the background and fluctuating magnetic fields. The solid vertical lines indicate the peak fluctuations around the crossing of the flux tube. The red-shaded area in panel (c) shows how the angle β changes with a smoothing parameter, that is, the length of the smoothing time interval changed from 0.6 to 3.6 min.

case of the last flybys which were significantly closer to Titan, the split signature appears at the altitude range from 1,580 km to 3,500 km. This observation could mean that the splitting of the magnetotail lobes become more significant at mid-range distances, while closer to Titan the magnetotail is confined into a continuous region. This is consistent with hybrid simulations by Modolo et al. (2007) and Kallio et al. (2007).

The observed current sheet in the T122 flyby most likely stems from the boundary layer between adjacent anti-parallel magnetotail lobes. This current sheet is found fairly close to the ionosphere and accompanied by a local density peak, indicating a possible pressure balance between magnetic and thermal pressure. In Figure 2e the pressure balance is not observed, meaning a larger contribution of the thermal electron and ion populations in this region (both electron and ion measurements included in this analysis are limited to the cold ionospheric electrons). It is hard to estimate the thickness of the current sheet due to the absence of bulk plasma velocity measurements. An assumption that the magnetotail current sheet is steady with respect to the spacecraft is not supported by the observations on other planets (e.g., Sergeev et al., 1998). On the contrary, this is a highly dynamic region with various types of bulk motion. Thus, the assumption that temporal measurements can be transformed into spatial measurements, is not valid for the T122 flyby and the ones following.

Before proceeding with the discussion, one has to analyze the current system and the possible sources of the current. In the moving with Titan frame of reference the corotational electric field $\mathbf{E} = -\mathbf{v} \times \mathbf{B}$ is creating currents in Titan's ionosphere. Due to the current density conservation $\nabla \cdot \mathbf{j} = 0$, the currents in a stationary case have to establish a closure in Titan's ionosphere. Thus the cross-tail current in the magnetotail current sheet observed during the T122 flyby eventually closes in Titan's ionosphere. At the same time, another type of current associated with the standing Alfvén wave exists. The Alfvén waves propagate away from Titan along the magnetic field lines

3.4. Draping Pattern: Summary of All Cassini's Flybys Near Titan

We applied the same technique for identifying the upstream magnetic field but automatically for each of the 126 flybys conducted during the Cassini mission. The measurements from the upstream/ramside were excluded from the analysis to avoid biasing of the result. Time intervals ± 1 hr around the closest approach were chosen to ensure that the magnetic field measurements were made outside the perturbed interaction region. However, due to the high upstream variability, an additional criterion was introduced. In Figure 6a the statistics of the angle α between the inbound and outbound magnetic field is plotted. The dashed line indicates the threshold angle of 20° (as a rather conservative threshold), which indicates when a particular flyby should be excluded from the analysis. This criterion removed almost half of the flybys.

In Figure 6b, the draping component of the magnetic field in the BFA frame is shown as if the magnetotail is pointing away from the plane of figure. A clear draping pattern of the magnetic field around Titan is observed. While sparse, the data coverage is deemed enough to qualitatively say that the draping occurs in a confined area of roughly $\sim 4 R_T$ along Y_{BFA} . The geometrical constraints on the draping boundary estimated by Neubauer et al. (2006) suggest an elliptical shape with semi-major and semi-minor axis in YZ plane to be ~ 2.0 and $\sim 3.5 R_T$ respectively (although these geometrical constraints were introduced for a cross-section of the magnetotail along $X_{TIS} = 1.2 R_T$, while Figure 6b shows the cross-section at $X_{BFA} > 0 R_T$).

4. Discussion

The observed variability of the magnetotail region is consistent with previously analyzed flybys (e.g., Simon et al., 2014). The studied flybys in Coates et al. (2012), T9, T63 and T75, reveal the presence of a split ion tail and filaments of the magnetic field in the magnetotail region downstream of Titan. Though it was reported that these signatures appear due to the upstream variations and formation of Alfvén wings, it is unclear if these features are permanent or just transient phenomena. Importantly, the split signature in the tail region was described for the mid-range flybys like T9, T63 and T75. In the

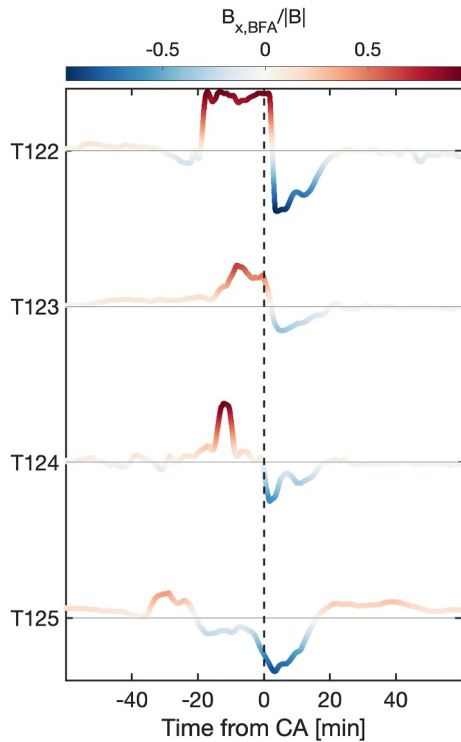


Figure 5. The non-background magnetic field component of the magnetic field during T122-T125 Cassini flybys. From the top to the bottom for each flyby, the deviations from the background magnetic field direction are color-coded. The arrows show the spreading of the magnetotail lobes: the solid lines correspond to the observed, and the dashed line is a mirrored solid line.

in both parallel and anti-parallel directions, and when encountering a plasma density gradient they either reflect or transmit through. Such density gradient can be the equatorial plasma sheet or Saturn's ionosphere, and it mediates the strength of the interaction. During the T122-T125 flybys Titan was located primarily in Saturn's magnetospheric lobes, thus we assume that the generated Alfvén waves don't encounter density gradients along the path. If the reflected from Saturn's polar ionosphere Alfvén waves propagate back to Titan, then the closure of currents is achieved and the interaction is strong, otherwise, Titan is decoupled from Saturn's ionosphere.

We estimate roughly the travel time of the Alfvén waves $\tau_A = 2L/V_A$, where L is the distance from Titan to Saturn and $L \approx 20 R_S$, V_A is the local Alfvén speed. The shift time $\tau_c = R_T/V_c$, where V_c is the corotational speed. The current closure is possible if the travel time of the Alfvén waves τ_A is less than the time τ_c that Titan needs to move a distance R_T along its orbit. Assuming that the Alfvén speed doesn't change along the magnetic field line and $\tau_A \leq \tau_c$, we get the requirement for a strong interaction $M_A = V_c/V_A \leq R_T/2L \approx 0.001$. If according to Arridge et al. (2011), the average upstream parameters in the magnetosphere ($|B| \approx 4.1$ nT, $n = 0.029$ m⁻³ from Table 3), the Alfvén Mach number $M_A = 0.6$. Therefore Titan is decoupled from Saturn. This indicates that the far-field region (a few R_T away from Titan) is characterized by local characteristics of an Alfvén wave, similar to the case of a weak interaction at Io (Neubauer, 1980) and doesn't depend on the conductivity of Saturn's ionosphere. In this case, the flux tube is bounded by the currents not necessarily field-aligned but rather aligned to the Alfvén wave characteristic.

The observational features of the Alfvén wing in the far-field include the perturbation of the transverse components of the background magnetic field and the presence of currents when crossing the flux tube. In the T123-T125 flybys, the magnetotail's neutral current sheet crossing is less pronounced, indicating a spreading of the flux tube. Instead, local perturbations of the

transverse components of the magnetic field at the surface of the magnetotail lobe/flux tube are observed as shown in Section 3.2 for T124 flyby (see Figure 4). The field-aligned currents can describe the observations if the fluctuations are locally transverse to the background magnetic field. Above 1,500 km the presence of perpendicular currents to the magnetic field (due to Pedersen and Hall conductivity) is negligible and it can be assumed that the parallel conductivity is predominant (Rosenqvist et al., 2009; Ågren et al., 2011). The same boundary

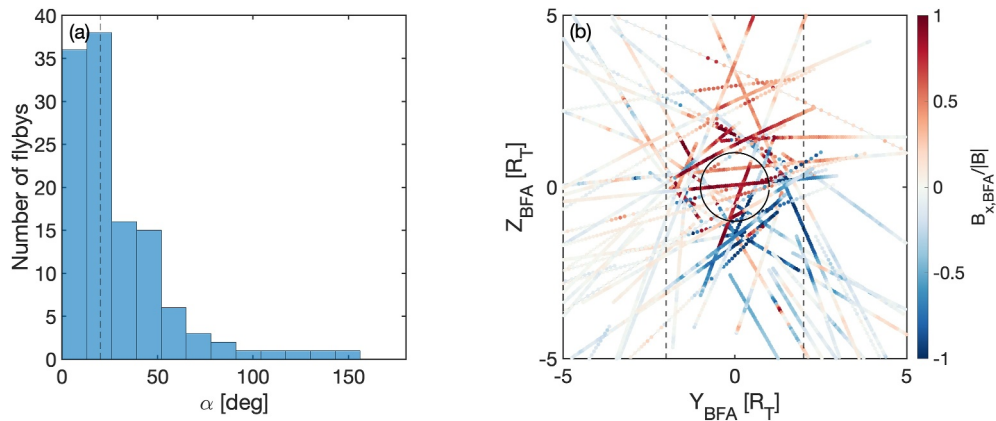


Figure 6. The draping pattern in the BFA reference frame. In panel (a) the calculated angle α between inbound and outbound. This parameter defines if it is possible for a particular flyby to transform magnetic field data into a BFA reference frame. The vertical dashed line is an arbitrary set threshold in such a way if the angle between the inbound and outbound legs exceeds the threshold, then it is not taken into account. In panel (b) the draped magnetic field component is shown for $X_{BFA} > 0 R_T$.

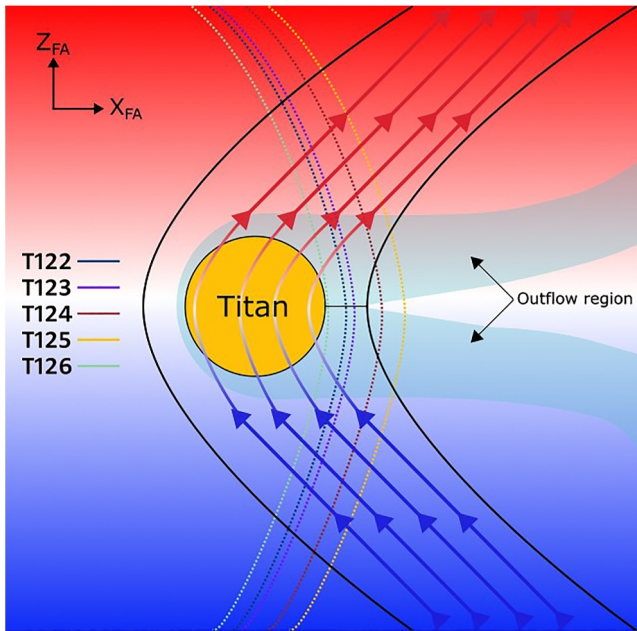


Figure 7. The artistic representation of Cassini flybys near Titan and the possible magnetotail configuration during T122-T126 flybys. The field lines of the magnetic field are shown in the BFA reference frame, so as the spacecraft trajectory. The color coding represents the evolution of Cassini's trajectory through Titan's magnetotail region. The magnetic field lines bent around Titan as they corotate with Saturn, which leads to the formation of Alfvén wings-like structure and outflow of ionospheric plasma.

currents are observed during T123 at the edge of magnetotail lobes, but somewhat weaker compared to T124. Therefore we conclude that throughout the last five flybys, Cassini consequently passes near the stem of Titan's Alfvén wings as demonstrated in Figure 7. The T125 and T126 flybys do not reveal any obvious magnetotail crossing.

The detection of an Alfvén wing at Titan is of interest as it is a great example of moon-plasma interaction in the sub-alfvenic flow due to the hybrid scales of the interaction (for $|\mathbf{B}| \approx 4.1$ nT and $|\mathbf{V}| \approx 90$ km s⁻¹ the ion gyroradius ρ , e.g. $\rho_{H^+} \approx 230$ km, $\rho_{O^+} = 16\rho_{H^+} \approx 3,680$ km, which is comparable to the size of Titan). The distinguishing between an Alfvén wing, magnetotail lobe, and flux tube is loose, as it is a matter of terminology. In all cases, the interaction possesses similar characteristics: the flow is decelerated on the ramside and accelerated on the flanks, and the magnetic field is draped and bent around Titan. However, to keep a more generalized approach, we use Alfvén wings to describe the magnetic field structure in Titan's vicinity. The currents at Titan are not limited by field-aligned, Pedersen and Hall currents. Suppose the pressure gradient in the ionosphere, pick-up, and time-varying electric field are non-negligible. In that case, diamagnetic, pick-up, and polarization currents might arise, similar to that described at Io (Goertz, 1980). In addition, the asymmetry in the electron number density distribution seen when crossing magnetotail lobes/Alfvén wings is possibly caused by the dayside-nightside asymmetry in the electron production rate.

In all cases, when measurements allow it, the cold ionospheric outflow is observed simultaneously with the enhanced magnetic field region. It is unclear how this plasma appears in this region without proper measurements of the particle distribution function, thus this question is left for future exploration. One could explain this region as just field-aligned electrons moving

along the field lines. Another possible way is the bulk acceleration due to magnetic tension along with magnetic mirror force acceleration as described by, for example, Edberg et al. (2011) and Romanelli et al. (2014). The $\mathbf{J} \times \mathbf{B}$ forces due to bent geometry apply extra forces onto ionospheric ions and consequently accelerate them tailwards.

To estimate the outflow rate of the cold plasma from Titan, we can use an ideal MHD approximation. The outflow rate Q is the number of particles per second crossing a surface and can be written as

$$Q = nVS, \quad (1)$$

where n is a number density [m⁻³], V is an outflow speed [m s⁻¹] and S is a tail's cross-section area [m²]. However, the flow velocity is unknown as direct measurements are unavailable. The near Titan plasma environment during the T122-T126 flybys, according to the classification of Kabanovic et al. (2017), mostly corresponds to lobe-like Saturn's magnetosphere. Therefore, the low- β plasma environment is assumed, and as a consequence pressure gradient terms are ignored. The density and velocity are assumed stationary (constant). The MHD momentum equation

$$\rho \left[\frac{\partial \mathbf{V}}{\partial t} + \mathbf{V} \cdot (\nabla, \mathbf{V}) \right] = \mathbf{J} \times \mathbf{B} - \nabla P, \quad (2)$$

where \mathbf{J} from Ampere's law is $\mu_0 \mathbf{J} = \nabla \times \mathbf{B}$ (ignoring displacement electric field). Substituting \mathbf{J} to Equation 2 and ignoring pressure gradient and time derivative, the resulting equation looks like

$$\rho \mathbf{V} \cdot (\nabla, \mathbf{V}) = \frac{\nabla \times \mathbf{B} \times \mathbf{B}}{\mu_0}. \quad (3)$$

The zeroth order of magnitude analysis of Equation 3 transforms it into an algebraic relation, where each value is changed to its characteristic value

$$\rho \mathbf{V} \cdot (\nabla, \mathbf{V}) = \frac{\nabla \times \mathbf{B} \times \mathbf{B}}{\mu_0} \rightarrow \frac{\rho_0 V_0^2}{L} \sim \frac{B_0^2}{L \mu_0} \rightarrow V_0 \sim \frac{B_0}{\sqrt{\mu_0 \rho_0}} \quad (4)$$

The order of magnitude analysis shows that plasma under $\mathbf{J} \times \mathbf{B}$ force in ideal time-stationary MHD flows with Alfvén velocity V_0 . For example, using Equations 1 and 4, and applying to T122 flyby (assuming quasi-neutrality, $n_i \sim n_e$, $n_i \sim 100 \text{ cm}^{-3}$, $\mathbf{B} \sim 5 \text{ nT}$), the Alfvén velocity $V_0 \sim 10.9 \text{ km s}^{-1}$, tail's cross-section $S_0 = \pi R_T^2$ results in an outflow rate $Q \sim 2.3 \cdot 10^{25} \text{ ions s}^{-1}$ for H^+ , which is consistent with, for example, Wahlund et al. (2005) and Coates et al. (2012).

5. Conclusions

In this study, the magnetotail structure during the last five Cassini Titan's flybys T122-T126 is analyzed. These flybys have similar flyby geometry, which allows for analyzing the dynamical state of Titan's magnetotail and wake region. The magnetic field data from Cassini MAG is transformed into aligned to the background magnetic field reference frame to mitigate perturbations and compare flybys in the same reference frames. It was found that despite similar trajectories and upstream conditions, the magnetotail region possesses both temporal and spatial variations. The splitting of Titan's magnetotail into two separate lobes is the most pronounced in T124 starting from the distance of 3,260 km (1.3 R_T). Among these five flybys, during the T122 flyby, the confined magnetotail lobes with the developed neutral current sheet were observed. During the T123 and T124, the Alfvén wing-like structure in the magnetotail was observed, as well as cold ionospheric plasma. The T125 flyby was interpreted as a partial crossing of one of the magnetotail lobes, and T126 didn't show any magnetotail structure due to flyby geometry. The general draping pattern is in agreement with the draping boundary structure suggested by Neubauer et al. (2006). The results of the analysis are consistent with previously analyzed mid-range tail flybys (e.g., Simon et al., 2014), capturing different states of the magnetotail. The analysis of all the flybys shows the general draping pattern of the magnetic field lines and how it is confined within a narrow region of around $\sim 4 R_T Y_{BFA}$.

Data Availability Statement

All the data used in this study is available on the Planetary Data System/NASA on the Cassini RPWS and MAG subpages by choosing Saturn as a target planet (<https://pds-ppi.igpp.ucla.edu/>).

Acknowledgments

KK and NE acknowledge funding from the Swedish Research Council (Vetenskapsrådet) under contract 2020–03962. The authors are also grateful to SNSA or Swedish National Space Agency (formerly SNSB or Swedish National Space Board), who supported the implementation of the RPWS/LP instrument and operations onboard Cassini. Finally, the authors would like to thank two anonymous reviewers for leaving valuable comments and improving this paper.

References

- Ågren, K., Andrews, D. J., Buchert, S. C., Coates, A. J., Cowley, S. W. H., Dougherty, M. K., et al. (2011). Detection of currents and associated electric fields in Titan's ionosphere from Cassini data. *Journal of Geophysical Research (Space Physics)*, 116(A4), A04313. <https://doi.org/10.1029/2010JA016100>
- Ågren, K., Wahlund, J. E., Garnier, P., Modolo, R., Cui, J., Galand, M., & Müller-Wodarg, I. (2009). On the ionospheric structure of Titan. *Planetary and space. Sciences*, 57(14–15), 1821–1827. <https://doi.org/10.1016/j.pss.2009.04.012>
- Arridge, C. S., André, N., Bertucci, C. L., Garnier, P., Jackman, C. M., Németh, Z., et al. (2011). Upstream of Saturn and Titan. *Space Science Reviews*, 162(1–4), 25–83. <https://doi.org/10.1007/s11214-011-9849-x>
- Arridge, C. S., Khurana, K. K., Russell, C. T., Southwood, D. J., Achilleos, N., Dougherty, M. K., et al. (2008). Warping of Saturn's magnetospheric and magnetotail current sheets. *Journal of Geophysical Research (Space Physics)*, 113(A8), A08217. <https://doi.org/10.1029/2007JA012963>
- Backes, H., Neubauer, F. M., Dougherty, M. K., Achilleos, N., André, N., Arridge, C. S., et al. (2005). Titan's magnetic field signature during the first Cassini encounter. *Science*, 308(5724), 992–995. <https://doi.org/10.1126/science.1109763>
- Bertucci, C., Achilleos, N., Dougherty, M. K., Modolo, R., Coates, A. J., Szego, K., et al. (2008). The magnetic memory of Titan's ionized atmosphere. *Science*, 321(5895), 1475–1478. <https://doi.org/10.1126/science.1159780>
- Bertucci, C., Hamilton, D. C., Kurth, W. S., Hospodarsky, G., Mitchell, D., Sergis, N., et al. (2015). Titan's interaction with the supersonic solar wind. *Geophysical Research Letters*, 42(2), 193–200. <https://doi.org/10.1002/2014GL062106>
- Bertucci, C., Neubauer, F. M., Szego, K., Wahlund, J. E., Coates, A. J., Dougherty, M. K., et al. (2007). Structure of Titan's mid-range magnetic tail: Cassini magnetometer observations during the T9 flyby. *Geophysical Research Letters*, 34(24), L24S02. <https://doi.org/10.1029/2007GL030865>
- Burne, S., Bertucci, C., Sergis, N., Morales, L. F., Achilleos, N., Sánchez-Cano, B., et al. (2023). Space weather in the Saturn-Titan system. *The Astrophysical Journal*, 948(1), 37. <https://doi.org/10.3847/1538-4357/acc738>
- Chatain, A., Wahlund, J. E., Shebanits, O., Hadid, L. Z., Morooka, M., Edberg, N. J. T., et al. (2021). Re-analysis of the Cassini RPWS/LP data in Titan's ionosphere: 1. Detection of several electron populations. *Journal of Geophysical Research (Space Physics)*, 126(8), e28412. <https://doi.org/10.1029/2020JA028412>

- Coates, A. J., Wellbrock, A., Lewis, G. R., Arridge, C. S., Crary, F. J., Young, D. T., et al. (2012). Cassini in Titan's tail: CAPS observations of plasma escape. *Journal of Geophysical Research (Space Physics)*, *117*(A5), A05324. <https://doi.org/10.1029/2012JA017595>
- Dougherty, M. K., Kellock, S., Southwood, D. J., Balogh, A., Smith, E. J., Tsurutani, B. T., et al. (2004). The Cassini magnetic field investigation. *Space Science Reviews*, *114*(1–4), 331–383. <https://doi.org/10.1007/s11214-004-1432-2>
- Edberg, N. J. T., Ågren, K., Wahlund, J. E., Morooka, M. W., Andrews, D. J., Cowley, S. W. H., et al. (2011). Structured ionospheric outflow during the Cassini T55–T59 Titan flybys. *Planetary and Space Science*, *59*(8), 788–797. <https://doi.org/10.1016/j.pss.2011.03.007>
- Edberg, N. J. T., Andrews, D. J., Shebanits, O., Ögren, K., Wahlund, J. E., Opgenoorth, H. J., et al. (2013). Extreme densities in Titan's ionosphere during the T85 magnetosheath encounter. *Geophysical Research Letters*, *40*(12), 2879–2883. <https://doi.org/10.1002/grl.50579>
- Engelhardt, I. A. D., Wahlund, J. E., Andrews, D. J., Eriksson, A. I., Ye, S., Kurth, W. S., et al. (2015). Plasma regions, charged dust and field-aligned currents near Enceladus. *Planetary and Space Science*, *117*, 453–469. <https://doi.org/10.1016/j.pss.2015.09.010>
- Feyerabend, M., Simon, S., Motschmann, U., & Liuzzo, L. (2015). Filamented ion tail structures at Titan: A hybrid simulation study. *Planetary and Space Science*, *117*, 362–376. <https://doi.org/10.1016/j.pss.2015.07.008>
- Feyerabend, M., Simon, S., Neubauer, F. M., Motschmann, U., Bertucci, C., Edberg, N. J. T., et al. (2016). Hybrid simulation of Titan's interaction with the supersonic solar wind during Cassini's T96 flyby. *Geophysical Research Letters*, *43*(1), 35–42. <https://doi.org/10.1002/2015GL066848>
- Galand, M., Coates, A. J., Cravens, T. E., & Wahlund, J.-E. (2014). Titan's ionosphere. In I. Müller-Wodarg, C. A. Griffith, E. Lellouch, & T. E. Cravens (Eds.), *Titan: Interior, surface, atmosphere, and space environment* (pp. 376–418). Cambridge University Press. <https://doi.org/10.1017/CBO9780511667398.014>
- Garnier, P., Dandouras, I., Toubanc, D., Roelof, E. C., Brandt, P. C., Mitchell, D. G., et al. (2010). Statistical analysis of the energetic ion and ENA data for the Titan environment. *Planetary and Space Science*, *58*(14–15), 1811–1822. <https://doi.org/10.1016/j.pss.2010.08.009>
- Goertz, C. K. (1980). Io's interaction with the plasma torus. *Journal of Geophysical Research*, *85*(A6), 2949–2956. <https://doi.org/10.1029/JA085A06p02949>
- Gurnett, D. A., Averkamp, T. F., Schippers, P., Persoon, A. M., Hospodarsky, G. B., Leisner, J. S., et al. (2011). Auroral hiss, electron beams and standing Alfvén wave currents near Saturn's moon Enceladus. *Geophysical Research Letters*, *38*(6), L06102. <https://doi.org/10.1029/2011GL046854>
- Gurnett, D. A., Kurth, W. S., Kirchner, D. L., Hospodarsky, G. B., Averkamp, T. F., Zarka, P., et al. (2004). The Cassini radio and plasma wave investigation. *Space Science Reviews*, *114*(1–4), 395–463. <https://doi.org/10.1007/s11214-004-1434-0>
- Gustafsson, G., & Wahlund, J. E. (2010). Electron temperatures in Saturn's plasma disc. *Planetary and Space Science*, *58*(7–8), 1018–1025. <https://doi.org/10.1016/j.pss.2010.03.007>
- Kabanovic, S., Simon, S., Neubauer, F. M., & Meeks, Z. (2017). An empirical model of Titan's magnetic environment during the Cassini era: Evidence for seasonal variability. *Journal of Geophysical Research (Space Physics)*, *122*(11), 11076–11085. <https://doi.org/10.1002/2017JA024402>
- Kallio, E., Sillanpää, I., Jarvinen, R., Janhunen, P., Dougherty, M., Bertucci, C., & Neubauer, F. (2007). Morphology of the magnetic field near Titan: Hybrid model study of the Cassini T9 flyby. *Geophysical Research Letters*, *34*(24), L24S09. <https://doi.org/10.1029/2007GL030827>
- Modolo, R., Chanteur, G. M., Wahlund, J. E., Canu, P., Kurth, W. S., Gurnett, D., et al. (2007). Plasma environment in the wake of Titan from hybrid simulation: A case study. *Geophysical Research Letters*, *34*(24), L24S07. <https://doi.org/10.1029/2007GL030489>
- Morooka, M. W., Modolo, R., Wahlund, J. E., André, M., Eriksson, A. I., Persoon, A. M., et al. (2009). The electron density of Saturn's magnetosphere. *Annales Geophysicae*, *27*(7), 2971–2991. <https://doi.org/10.5194/angeo-27-2971-2009>
- Morooka, M. W., Wahlund, J. E., Eriksson, A. I., Farrell, W. M., Gurnett, D. A., Kurth, W. S., et al. (2011). Dusty plasma in the vicinity of Enceladus. *Journal of Geophysical Research (Space Physics)*, *116*(A12), A12221. <https://doi.org/10.1029/2011JA017038>
- Németh, Z., Szego, K., Bebesi, Z., Erdős, G., Foldy, L., Rymer, A., et al. (2011). Ion distributions of different Kronian plasma regions. *Journal of Geophysical Research (Space Physics)*, *116*(A9), A09212. <https://doi.org/10.1029/2011JA016585>
- Neubauer, F. M. (1980). Nonlinear standing Alfvén wave current system at Io: Theory. *Journal of Geophysical Research*, *85*(A3), 1171–1178. <https://doi.org/10.1029/JA085A03p01171>
- Neubauer, F. M. (1998). The sub-Alfvénic interaction of the Galilean satellites with the Jovian magnetosphere. *Journal of Geophysical Research*, *103*(E9), 19843–19866. <https://doi.org/10.1029/97JE03370>
- Neubauer, F. M., Backes, H., Dougherty, M. K., Wennmacher, A., Russell, C. T., Coates, A., et al. (2006). Titan's near magnetotail from magnetic field and electron plasma observations and modeling: Cassini flybys TA, TB, and T3. *Journal of Geophysical Research (Space Physics)*, *111*(A10), A10220. <https://doi.org/10.1029/2006JA011676>
- Omid, N., Sulaiman, A. H., Kurth, W., Madanian, H., Cravens, T., Sergis, N., et al. (2017). A single deformed bow shock for Titan-Saturn system. *Journal of Geophysical Research (Space Physics)*, *122*(11), 11058–11075. <https://doi.org/10.1002/2017JA024672>
- Regoli, L. H., Roussos, E., Dialynas, K., Luhmann, J. G., Sergis, N., Jia, X., et al. (2018). Statistical study of the energetic proton environment at Titan's orbit from the Cassini spacecraft. *Journal of Geophysical Research (Space Physics)*, *123*(6), 4820–4834. <https://doi.org/10.1029/2018JA025442>
- Romanelli, N., Modolo, R., Dubinin, E., Berthelier, J. J., Bertucci, C., Wahlund, J. E., et al. (2014). Outflow and plasma acceleration in Titan's induced magnetotail: Evidence of magnetic tension forces. *Journal of Geophysical Research (Space Physics)*, *119*(12), 9992–10005. <https://doi.org/10.1002/2014JA020391>
- Rosenqvist, L., Wahlund, J. E., Ågren, K., Modolo, R., Opgenoorth, H. J., Strobel, D., et al. (2009). Titan ionospheric conductivities from Cassini measurements. *Planetary and Space Science*, *57*(14–15), 1828–1833. <https://doi.org/10.1016/j.pss.2009.01.007>
- Rymer, A. M., Smith, H. T., Wellbrock, A., Coates, A. J., & Young, D. T. (2009). Discrete classification and electron energy spectra of Titan's varied magnetospheric environment. *Geophysical Research Letters*, *36*(15), L15109. <https://doi.org/10.1029/2009GL039427>
- Sergeev, V., Angelopoulos, V., Carlson, C., & Sutcliffe, P. (1998). Current sheet measurements within a flapping plasma sheet. *Journal of Geophysical Research*, *103*(A5), 9177–9187. <https://doi.org/10.1029/97JA02093>
- Shebanits, O., Wahlund, J. E., Edberg, N. J. T., Crary, F. J., Wellbrock, A., Andrews, D. J., et al. (2016). Ion and aerosol precursor densities in Titan's ionosphere: A multi-instrument case study. *Journal of Geophysical Research (Space Physics)*, *121*(10), 10075–10090. <https://doi.org/10.1002/2016JA022980>
- Simon, S., Neubauer, F. M., Wennmacher, A., & Dougherty, M. K. (2014). Variability of Titan's induced magnetotail: Cassini magnetometer observations. *Journal of Geophysical Research (Space Physics)*, *119*(3), 2024–2037. <https://doi.org/10.1002/2013JA019608>
- Simon, S., Wennmacher, A., Neubauer, F. M., Bertucci, C. L., Krieger, H., Russell, C. T., & Dougherty, M. K. (2010b). Dynamics of Saturn's magnetotail near Titan's orbit: Comparison of Cassini magnetometer observations from real and virtual Titan flybys. *Planetary and Space Science*, *58*(12), 1625–1635. <https://doi.org/10.1016/j.pss.2010.08.006>

- Simon, S., Wennmacher, A., Neubauer, F. M., Bertucci, C. L., Kriegel, H., Saur, J., et al. (2010a). Titan's highly dynamic magnetic environment: A systematic survey of Cassini magnetometer observations from flybys TA-T62. *Planetary and Space Science*, 58(10), 1230–1251. <https://doi.org/10.1016/j.pss.2010.04.021>
- Smith, H. T., & Rymer, A. M. (2014). An empirical model for the plasma environment along Titan's orbit based on Cassini plasma observations. *Journal of Geophysical Research (Space Physics)*, 119(7), 5674–5684. <https://doi.org/10.1002/2014JA019872>
- Szego, K., Bebesi, Z., Bertucci, C., Coates, A. J., Cray, F., Erdos, G., et al. (2007). Charged particle environment of Titan during the T9 flyby. *Geophysical Research Letters*, 34(24), L24S03. <https://doi.org/10.1029/2007GL030677>
- Wahlund, J. E., Boström, R., Gustafsson, G., Gurnett, D. A., Kurth, W. S., Pedersen, A., et al. (2005). Cassini measurements of cold plasma in the ionosphere of Titan. *Science*, 308(5724), 986–989. <https://doi.org/10.1126/science.1109807>
- Wahlund, J. E., Modolo, R., Bertucci, C., & Coates, A. J. (2014). Titan's magnetospheric and plasma environment. In *Titan: Interior, surface, atmosphere, and space environment* (p. 419). Cambridge University Press. <https://doi.org/10.1017/CBO9780511667398.015>
- Wei, H. Y., Russell, C. T., Dougherty, M. K., Ma, Y. J., Hansen, K. C., McAndrews, H. J., et al. (2011). Unusually strong magnetic fields in Titan's ionosphere: T42 case study. *Advances in Space Research*, 48(2), 314–322. <https://doi.org/10.1016/j.asr.2011.02.009>
- Wei, H. Y., Russell, C. T., Wahlund, J. E., Dougherty, M. K., Bertucci, C., Modolo, R., et al. (2007). Cold ionospheric plasma in Titan's magnetotail. *Geophysical Research Letters*, 34(24), L24S06. <https://doi.org/10.1029/2007GL030701>
- Young, D. T., Berthelier, J. J., Blanc, M., Burch, J. L., Coates, A. J., Goldstein, R., et al. (2004). Cassini plasma spectrometer investigation. *Space Science Reviews*, 114(1–4), 1–112. <https://doi.org/10.1007/s11214-004-1406-4>